On the geodynamics of the northern Adriatic plate

RENDICONTI LINCEI
SCIENZE FISICHE E NATURALI

ISSN 2037-4631
Volume 21
Supplement 1

Rend. Fis. Acc. Lincei (2010)
21:253-279
DOI 10.1007/
s12210-010-0098-9

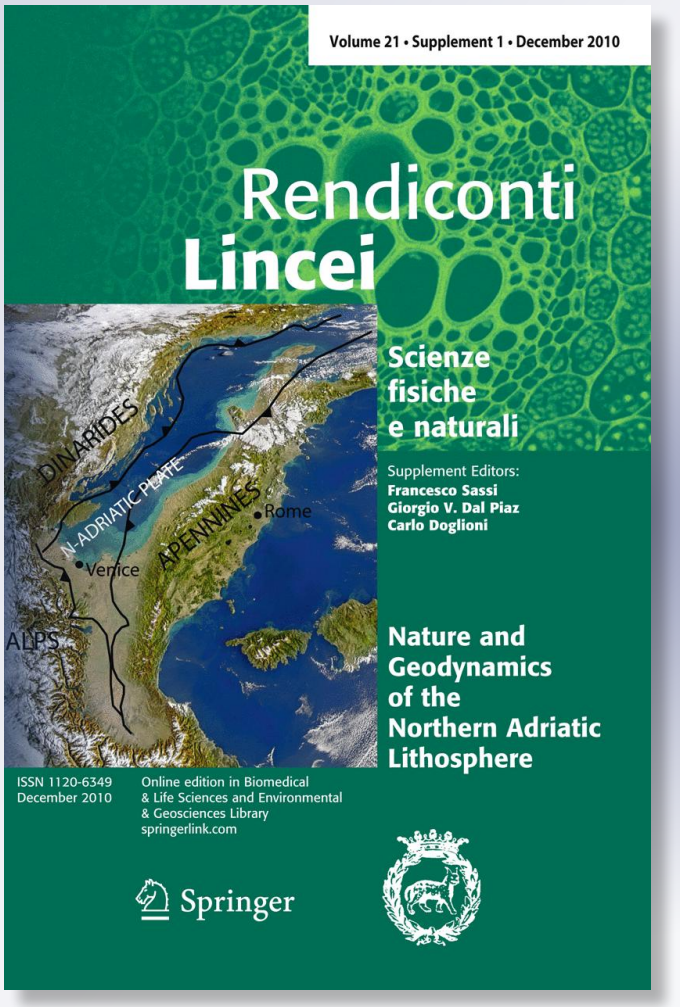

Springer

Rend. Fis. Acc. Lincei (2010) 21 (Suppl 1):S253–S279
DOI 10.1007/s12210-010-0098-9

On the geodynamics of the northern Adriatic plate

Marco Cuffaro · Federica Riguzzi · Davide Scrocca · Fabrizio Antonioli · Eugenio Carminati · Michele Livani · Carlo Doglioni

Received: 22 December 2009 / Accepted: 22 September 2010 / Published online: 22 October 2010

Abstract The northern Adriatic plate underwent Permian-Mesozoic rifting and was later shortened by three orogenic belts (i.e., Apennines, Alps and Dinarides) developed along three independent subduction zones. The inherited Mesozoic horst and graben grain determined structural undulations of the three thrust belts. Salients developed in grabens or more shaly basins, whereas recesses formed regularly around horsts. A new interpretation of seismic reflection profiles, subsidence rates from stratigraphic analysis, and GPS data prove that the three orogens surrounding the northern Adriatic plate are still active. The NE-ward migration of the Apennines subduction hinge determines the present-day faster subsidence rate in the western side of the northern Adriatic (>1 mm/year). This is recorded also by the SW-ward dip of the foreland regional monocline, and the SW-ward increase of the depth of the Tyrrhenian sedimentary layer, as well as the increase in thickness of the Pliocene and Pleistocene sediments. These data indicate the dominant influence of the Apennines subduction, which controls the asymmetric subsidence in the northern Adriatic realm. The Dinarides front has been tilted by the Apennines subduction hinge, as shown by the eroded Dalmatian anticlines subsiding in the eastern Adriatic Sea. GPS data suggest that southward tilting of the western and central Southern Alps, whereas the eastern Southern Alps are uplifting. The obtained strain rates are on average within 20 nstrain/year. The horizontal

The original version of this paper was presented in Venice (November 5–6, 2009) at the Meeting "Nature and geodynamics of the lithosphere in Northern Adriatic" sponsored by the Accademia Nazionale dei Lincei, Accademia Nazionale delle Scienze detta dei XL and Istituto Veneto di Scienze, Lettere ed Arti.

M. Cuffaro · E. Carminati · M. Livani · C. Doglioni
Dipartimento di Scienze della Terra, Sapienza Università di Roma, Rome, Italy

M. Cuffaro (✉) · D. Scrocca · E. Carminati · M. Livani · C. Doglioni
Istituto di Geologia Ambientale e Geoingegneria (IGAG), CNR, c/o Dipartimento di Scienze della Terra, Sapienza Università di Roma, P.le A. Moro 5, PO Box 11, 00185 Rome, Italy
e-mail: marco.cuffaro@uniroma1.it

F. Antonioli
ENEA, Casaccia, Rome, Italy

F. Riguzzi
Istituto Nazionale di Geofisica e Vulcanologia, Rome, Italy

shortening obtained from GPS velocities at the front of the three belts surrounding the northern Adriatic plate are about 2–3 mm/year (Northern Apennines), 1–2 mm/year (Southern Alps), and <1 mm/year (Dinarides). The shortening directions tend to be perpendicular to the thrust belt fronts. The areas where the strain rate sharply decreases along a tectonic feature (e.g., the Ferrara salient, the Venetian foothills front) are proposed to be occupied by locked structures where stress is accumulating in the brittle layer and thus seismically prone. Finally, we speculate that, since the effects of three independent subduction zones coexist and overlap in the same area, plate boundaries are passive features.

Keywords Adriatic plate · Plate boundaries · Thrust tectonics · Subsidence · Geodetic strain rate

1 Introduction

The Northern Adriatic Sea is an ideal area to integrate a large number of information deriving from geological and geophysical investigations. A wealth of stratigraphic data, seismic reflection profiles, historical and instrumental seismicity, and space geodesy form a rather complete data set that allows us to reconstruct the evolution of this element of the Mediterranean lithosphere. The study area represents a Tethyan stretched passive continental margin during the Permian-Mesozoic. The area, located in the northern part of the so-called Africa promontory (sensu Argand 1924), was possibly an independent plate (Adriatic plate, also named Apulia or Adria) from the Africa plate when the Ionian basin opened during the Mesozoic(?) as proposed by Catalano et al. (2001). During the Cenozoic, the Adriatic plate was involved in the Apennines, Alpine, and Dinarides subduction zones, respectively surrounding its western, northern, and eastern margins. The goal of this research is threefold, i.e., (1) to summarize the main tectonic history of the study area, monitoring the seismic risk; (2) to present new interpretations of seismic lines, new GPS data and a new subsidence study based on stratigraphic and GPS data, illustrating how the northern Adriatic Plate is still a very active realm; and (3) to show the superposition of different geodynamic mechanisms in the same area, supporting a passive origin of plate boundaries, contrary to what is usually assumed.

2 Tectonic setting

The northern Adriatic is the foreland area of three different orogens, i.e., the Apennines, the Alps, and the Dinarides (Fig. 1). In fact, it represents the foredeep and foreland of the SW-directed Apennines subduction (Carminati et al. 2003), the retrobelt foreland of the SE-directed Alpine subduction (Doglioni and Carminati 2002; Dal Piaz et al. 2003; Kummerow et al. 2004), and the foreland basin of the NE-directed Dinaric subduction (Di Stefano et al. 2009).

When reconstructing the Tethyan rifting evolution of the area, clear Permian and Triassic subsidence is recorded, with a fast acceleration during the Late Triassic?—Early Jurassic rifting (Bertotti et al. 1993; Carminati et al. 2010a). Subsidence at later time has been explained as due to thermal cooling induced by lithospheric stretching (e.g., Winterer and Bosellini 1981; Bertotti et al. 1997). The stretching associated with the Mesozoic horst and graben development brought to the development of portions of the Adriatic lithosphere characterized by different rehology profiles that potentially led to a rheological control

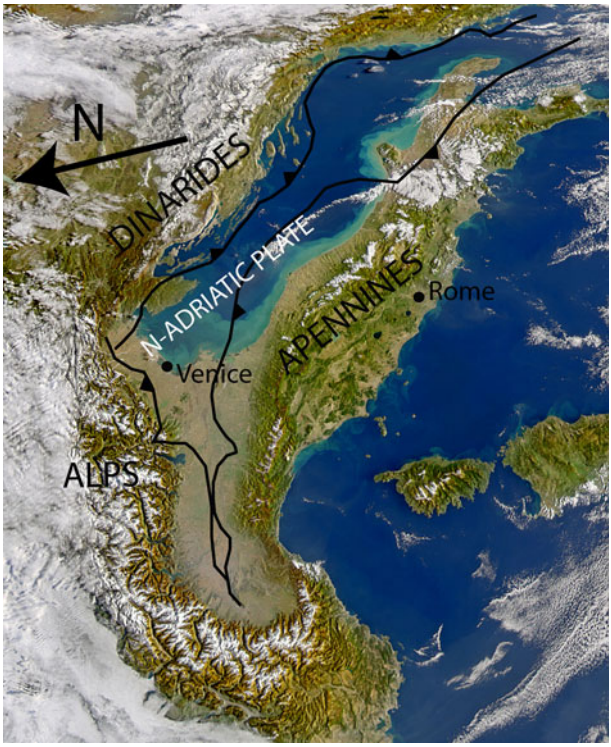

Fig. 1 Nasa Space Shuttle picture of the study area, with the location of the northern Adriatic plate surrounded and deformed by the Dinarides, Alps, and Apennines subduction zones. The undeformed part of the N-Adriatic Plate refers to the Padane-Adriatic Foreland in the Structural Model of Italy (Bigi et al. 1990)

during the subsequent foreland basin evolution (Bertotti et al. 1998). Syn- and post-rift subsidence rates vary as a function of the thinning of the crust and the consequent generation of horsts and grabens (Fig. 2). This is well constrained by the Permo-Mesozoic thickness variation (e.g., comparing the eastern Dolomites with the northern Adriatic). These two areas underwent uplift (producing the Dolomites mountains) during the Cenozoic when they were incorporated into the retrobelt of the Alps, while the northern-central Adriatic rather subsided very fast (>1 mm/year), being located in the foreland of the Apennines retreating subduction (Fig. 3).

The Mesozoic horsts and grabens are characterized by thinner and thicker sedimentary sequences respectively, sometimes coinciding with shallow and deep water sedimentary facies (e.g., Winterer and Bosellini 1981). This lithospheric stretching developed on a lithosphere previously thickened by the Carboniferous Hercynian orogen (e.g., Vai 1979). The rifting produced relevant lateral variations in the crustal thickness and in the stratigraphy and hence in the rheology of basement rocks and sedimentary successions (e.g., Bertotti et al. 1997; Carminati et al. 2010a). Therefore, during the shortening associated with the centripetally converging Apennines, Southern Alps and Dinarides fold and thrust belts, the inherited structural anisotropies controlled the development of undulations such as salients in the basins, and recesses in the horst. For example, the salients and recesses of the buried northern Apennines beneath the Po Basin appear controlled by the

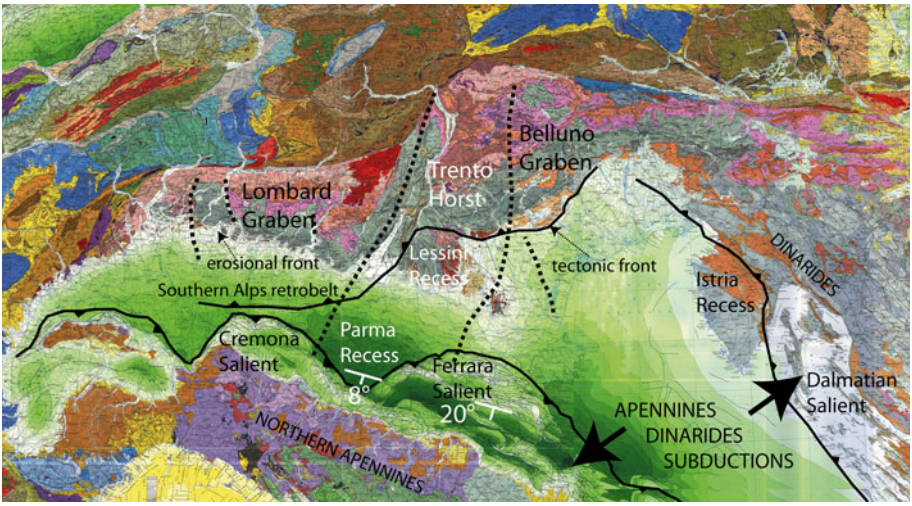

Fig. 2 Structural Model of Italy (after Bigi et al. 1990). The salients and recesses of the Apennines accretionary prism follow the inherited structure of the Permo-Mesozoic rifting that generated the Lombard Graben, the Trento Horst, and the Belluno Graben. Similar undulations can be recognized at the alpine and dinaric front. Note the different morphology of the Southern Alps foothills which is and erosional front in the western segment, whereas it follows the tectonic lineaments along the eastern side. To the west, the tectonic front of the Southern Alps is buried under the Po Basin because it has been southerly tilted by the Apennines slab retreat

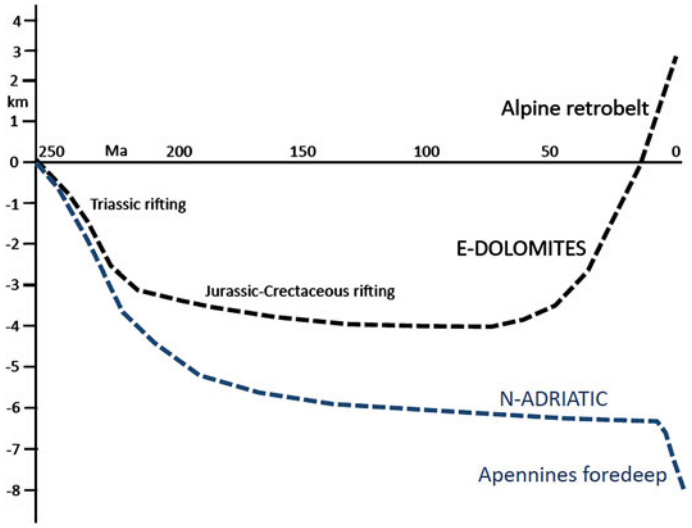

Fig. 3 Interpretation of the vertical evolution in the eastern Dolomites and in the central-northern Adriatic Sea. After a fast Triassic subsidence, the tectonic and thermal subsidence continued into the Jurassic and Cretaceous in both areas, although with locally different rates. During the Cenozoic the Southern Alps have been uplifted as the retrobelt of the Alps, whereas the Adriatic Sea and the Po Basin have been rapidly sinking being located in the foredeep of the Apennines subduction system

southward prolongation of the Southern Alps grabens and horsts (Fig. 2). Moving along strike, the foreland regional monocline of the Apennines shows variable angles, where the shallower values occur at the intersection with inherited horsts, and steeper angles are at the intersection with grabens (Fig. 2). The Mesozoic horsts have thinner sedimentary sequences with respect to the adjacent grabens. Therefore in the grabens, where the syn-tectonic sequences are thicker and the basal decoupling is generally deeper, the spacing between thrust planes is wider, i.e., a salient occurred. Viceversa, in correspondance with Mesozoic horsts, the shallower basement-cover transition produced a more superficial decollement and shorter thrust spacing, i.e., a recess developed (Fig. 4). In fact the Cremona salient propagated into the Lombard Graben-basin to the north; the Parma recess developed at the encroachment with the Trento Horst, whereas the Ferrara salient or arc occurs along the southern propagation of the Belluno Graben (Carminati et al. 2010b). This is a tectonic terminology, since we are defining horst and gaben as controlling thickness variations, rather than lateral facies (e.g., Trento Platform and Belluno Basin). In fact, in the Ferrara 1 well, located at the northwestern margin of the Ferrara Salient, the Mesozoic in the hangingwall is thicker than the footwall, regardless that the same Trento Platform sedimentary sequence is found both above and below the thrust. This indicates that the hangingwall pertains to the more subsided Belluno Graben rather than to the typical Trento Horst.

Apennines, Alps, and Dinarides are currently active, although at different rates (D'Agostino et al. 2005; Devoti et al. 2008). Each subduction is associated with different vertical motions, e.g., subsidence in the foreland basin and uplift in the belt. All three belts propagated toward the Adriatic lithosphere (Panza et al. 1982, 2003, 2007; Panza and Raykova 2008), gradually reducing the area of the plate (Fig. 5).

The northern Adriatic is contemporaneously undergoing the effects of three independent subduction zones that surround it (Fig. 5), and only a limited area of the plate is untouched by the compressive features (Figs. 1, 6). In northeastern Italy, Alps and Dinarides developed, overlapping and cross-cutting each other, during the Cenozoic (Fig. 5). Contrary to what previously proposed (Doglioni 1987), the Dinaric front in the Southern Alps could be

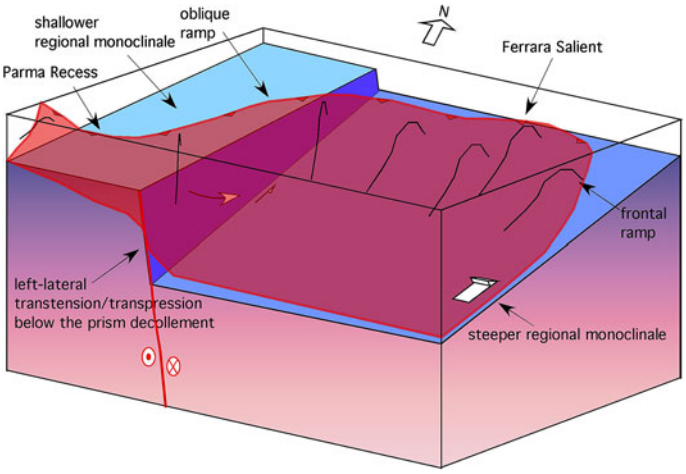

Fig. 4 Schematic model at the transition between the Ferrara salient and the Parma recess. The salient occurs where the regional monocline is steeper, the decollement is deeper, and the distance between thrust ramps is wider with respect to the adjacent shallower basement dip

more restricted to its easternmost part (Doglioni and Carminati 2008). In this recent view (Fig. 7), the WSW-vergent thrusts of the Dolomites are rather interpreted as structures developed in the transfer zone between the recess of the early alpine retrobelt thrusting on the Trento Horst, and the Belluno graben salient, similarly to that observed more to the west between the Trento Horst and the Lombardy graben (Fig. 7). The later deepening of the thrusts may explain the tilting and deactivation of the shallow structures in the Dolomites (Fig. 8). In addition, the recognition of widespread SW verging thrusts led Castellarin et al. (1992) to propose the occurrence of a Late Oligocene-Early Miocene NE–SW shortening phase.

Among the three belts, the Apennines developed along the only subduction where the slab hinge is migrating away relative to the upper plate (Alps and Dinarides have rather the subduction hinge moving toward the upper plate). This kinematic character is typical of W-directed subductions, where fast (>1 mm/year) subsidence rate in the depocenter of the

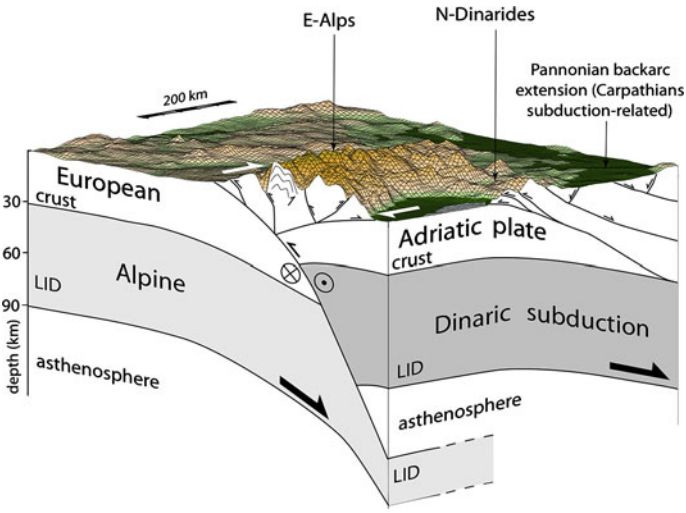

Fig. 5 3D reconstruction at the interference between the Alpine and Dinaric subductions in northeastern Italy, along the northeastern border of the Adriatic plate. Extension of the Pannonian, Carpathians subduction-related back-arc basin crosscut Eastern Alps and northern Dinarides. The area is also undergoing far field subsidence related to the retreat of the Apennines subduction

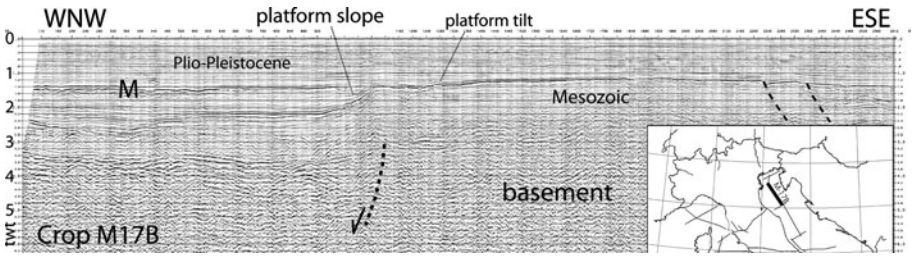

Fig. 6 Seismic reflection profile M17B in the central-northern Adriatic showing the clinoformed margin of the Mesozoic-Eocene(?) carbonate platform. Note the underlying hypothesized synsedimentary normal fault and the northward tilted slope of the carbonate platform backreef. *M* Messinian

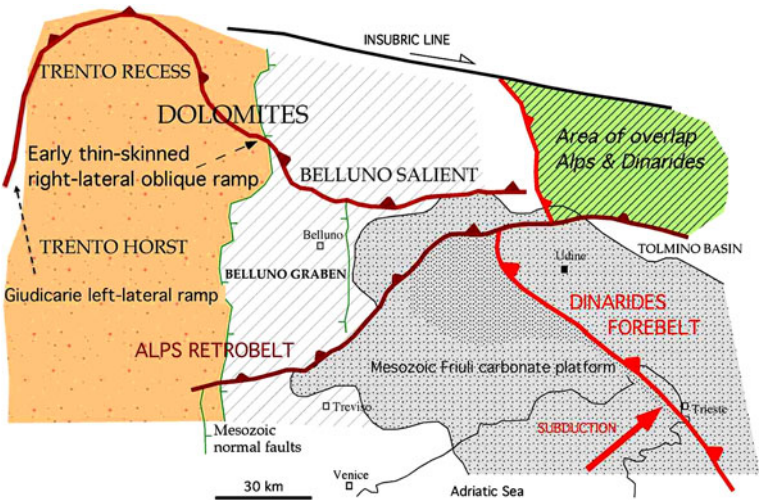

Fig. 7 The WSW-verging thrusts in the Dolomites are here interpreted as the oblique right-lateral transpressive ramp of the advancing Eocene alpine thrusting between the Trento recess and the Belluno salient. The left-lateral transpression in Giudicarie belt is considered as the conjugate ESE-verging counterpart, along the western margin of the salient, along the Trento Horst–Lombard Graben transition. In this interpretation the area of Alps–Dinarides overlap is confined in the eastern part of the Southern Alps (after Doglioni and Carminati 2008)

foredeep basin also occurs (Doglioni et al. 2007). In fact, the wedge of Pleistocene foredeep sediments thickens moving from NE to SW toward the Apennines (Fig. 9). The variable dip of the regional monocline (e.g., moving from NE to SW, from close to 0° in the Friuli far foreland, about 1.5° around Venice, up to more than 20° beneath Bologna) mimics the asymmetric subsidence, and testifies for the steepening of the lithospheric top when moving toward the subduction hinge (Fig. 10). The pinch-out of the lower Pleistocene sediments points for syn-tectonic deposition. The upper Pleistocene sediments are characterized by progradational patterns related mainly to the deltas of the Alpine rivers. Such clinoforms in the Pleistocene sediments could suggest a filling of a pre-existing basin, claiming for lower or absent subsidence rates during that time frame. However, the faster subsidence recorded by the Tyrrhenian sedimentary layer (MIS 5.5; ca. 125 kyr) toward the Apennines confirms the whole Pleistocene record, highlighting an asymmetric subsidence.

Therefore, in spite of the three competing subductions acting along the northern Adriatic plate boundaries, the flexure of the Apennines slab controls almost completely the subsidence of the northern Adriatic area (Carminati et al. 2003, 2005). The northeastward migration of the hinge of the northern Apennines subducting plate determines a corresponding trend in subsidence rates, which decrease moving toward the foreland from >1 mm/year, to less than 0.5 mm/year (Fig. 11). The Dinarides front has been shown to be active both from surface, seismic reflection and seismological data (e.g., Merlini et al. 2002; Galadini et al. 2005). The Southern Alps front is also notoriously very active as proved by seismicity (Bressan et al. 1998; Slejko et al. 1999) and geological and geophysical evidence (Doglioni 1992a; Galadini et al. 2005; Castellarin et al. 2006).

The Dinarides have been tilted by the down-flexure of the Adriatic plate, and the thrust-belt front, after being sub-aerially eroded, has been subsided (Fig. 12). This is consistent with the thinning toward the east of the Pliocene–Pleistocene sediments in the Adriatic

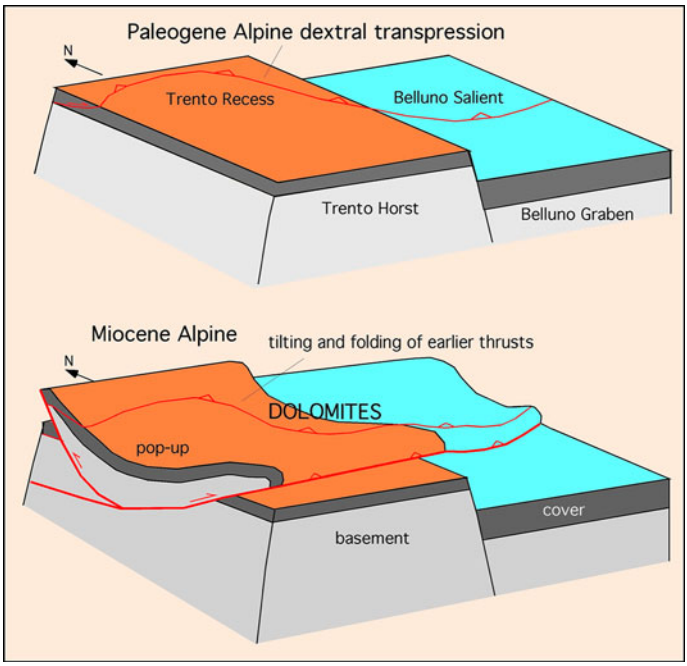

Fig. 8 The earlier alpine deformation inherited the Trento Horst determining a recess on the structural high and a salient in the adjacent graben. The transfer zone to the Belluno Basin consists of right-lateral transpression with thin-skinned WSW-verging thrusts. The later deeper thickskinned deformation, involving the basement, generated the Dolomites pop-up, folding and tilting the earlier shallower thrusts

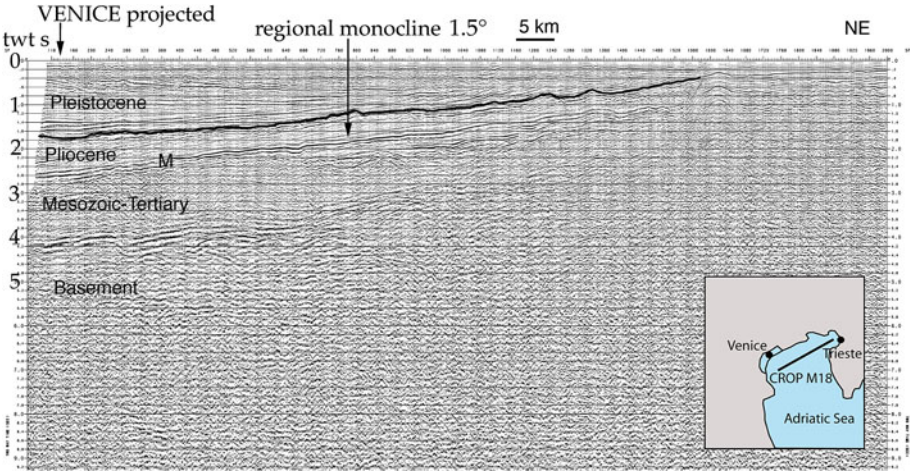

Fig. 9 Seismic reflection profile (CROP M-18) of the northern Adriatic Sea. Note the regional dip of the basement and the overlying cover up to the Pliocene dipping toward the southwest (location in Fig. 10). The lower part of the Pleistocene sediments show pinch-out geometries moving northeastward, indicating syntectonic deposition coeval to the differential subsidence in the underlying rocks. *M* Messinian unconformity. Vertical scale in seconds, two way time (after Carminati et al. 2003)

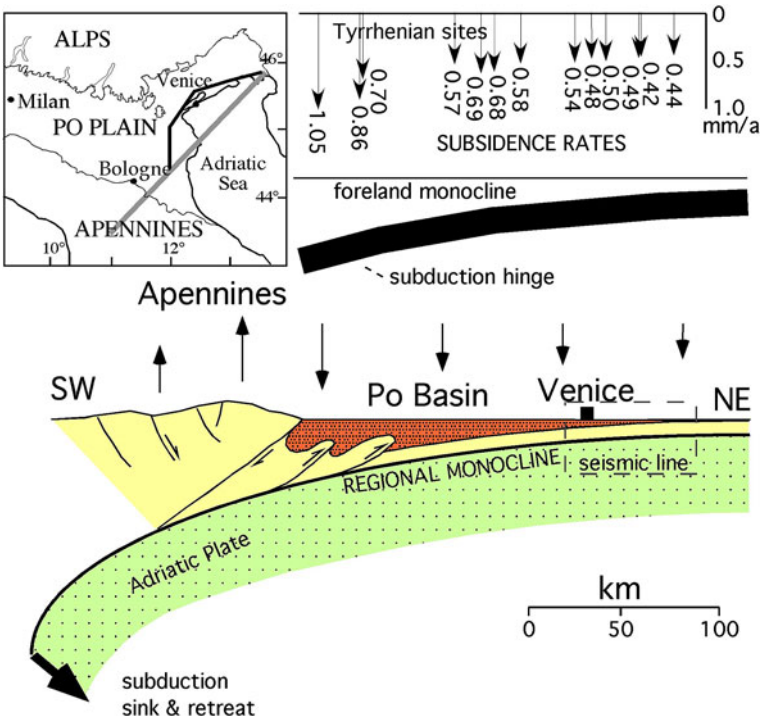

Fig. 10 Subsidence rates determined by the depth of the Tyrrhenian (MIS 5.5) layer cored mostly along the gray line running on the coast are displayed in the top panel (data after Antonioli et al. 2009). These rates indicate faster subsidence in the southwestern part of the profile, i.e., an asymmetric active subsidence, coherently with the independent data of the previous figure. The dip of the regional monocline in the northern Adriatic Sea recorded the faster subsidence to the southwest and it can be explained by the northeastward slab retreat of the Adriatic slab. The *dashed box* labeled as "seismic line" shows the position in this profile of the cross-section shown as Fig. 9

Sea, and the subsidence of the previously eroded anticlines of the Dinarides front, as visible along the Dalmatian islands. In summary, the northern Adriatic is an area where three independent geodynamic mechanisms overlap. The coexistence in the same area of the effects of more than one plate boundary can be read as evidence that plate boundaries are passive features.

3 Northeastern Apennines front

The northern Apennines are the northern part of a long arc, running from Piemonte in northwestern Italy, throughout the central-southern Apennines and Calabria along the Italian peninsula, continuing down in Sicily and into the northern Africa Maghrebides. The Apennines have been interpreted as underlined by a shallow asthenosphere wedging at the subduction hinge and lying beneath the western side of the belt (e.g., Doglioni et al. 1999). This interpretation has been confirmed in a number of geophysical and geological investigations (e.g., Picotti and Pazzaglia 2008). The retreat of the Apennines slab has been interpreted as the evidence for the slab pull (Royden 1993). However, the Adriatic plate is continental, and its density is lower than the underlying mantle. Therefore, the positive

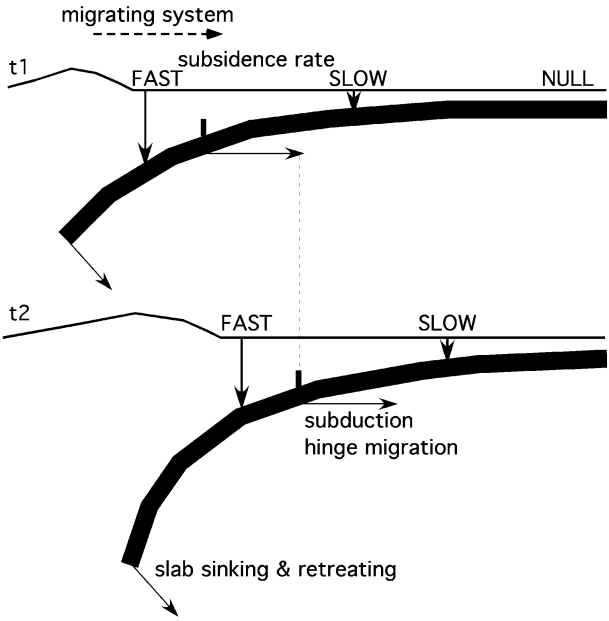

Fig. 11 Model of the migration of the subsidence rates which decrease moving toward the foreland of the subduction. As the subduction hinge retreats toward the foreland, the subsidence rate increases

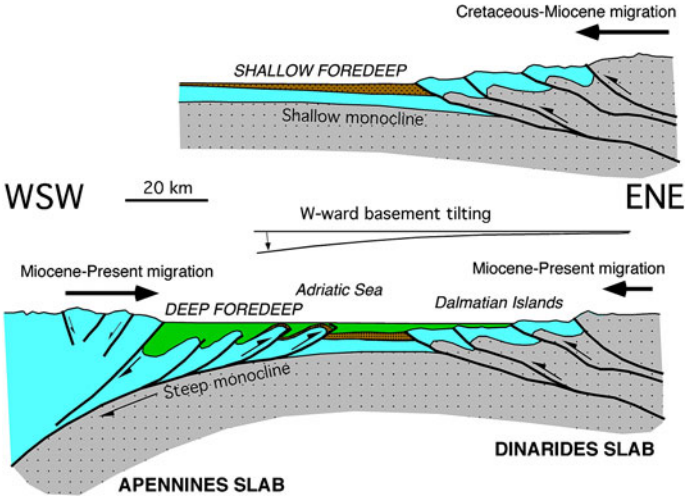

Fig. 12 Schematic cross section from the western to the eastern Adriatic Sea showing the two accretionary prisms at the front of the Apennines and Dinarides subduction zones. The Dinarides are older and slower, and they have been downward tilted by the regional monocline of the Apennines subduction hinge retreat

buoyancy of the Adriatic slab cannot explain the foundering of the subduction. Alternatively, the retreat of the slab for west-directed subduction zones has been interpreted as related by the easterly directed mantle flow, implicit with the notion of the westward drift of the lithosphere (Doglioni et al. 2007). The analysis of orogens related to west-directed

subduction zones (e.g., Doglioni et al. 1999) reveals the presence of an active accretionary wedge delimited at its footwall by the external thrust front and at its hangingwall by a thrust responsible for the rapid uplift of the chain which generally shows an "out-of-sequence" character. Recent studies have confirmed this interpretative scheme also for the central-northern portions of the Apennines (Basili et al. 2008; Montone et al. 2004; Scrocca et al. 2007; Carminati et al. 2010b). The accretion occurs at the expenses of the upper layers of the lower plate.

The geometry of the main thrusts in the central-northern Adriatic Sea has been described in several studies (among many others, Ori et al. 1986; Argnani et al. 1991; Casero et al. 1990; Consiglio Nazionale delle Ricerche 1992). Recently, a more external position of the Apennines thrust front in the central Adriatic domain, with respect to the commonly accepted interpretation, has been proposed by Scrocca (2006).

Apart from some conflicting interpretations regarding the thrust system architecture, the timing of contractional deformations is still debated. As an example, Di Bucci and Mazzoli (2002) proposed that thrusting and related folding in this area ceased in the Early Pleistocene, whereas the possible presence of seismogenic sources, all along the front of the northern-central Apennines, has been proposed by other researchers (Benedetti et al. 2003; Basili et al. 2008; Picotti and Pazzaglia 2008; Wegmann and Pazzaglia 2009; Wilson et al. 2009). These sources may explain the instrumental seismicity recorded in the area (Castello et al. 2006) and also some historical earthquakes (e.g., 23 December 1690 "Anconetano" earthquake), although a direct link between structures and seismicity is prevented by the errors associated with the depth localization of the seismic events.

In this contribution the geometry of the main thrust surfaces has been investigated by integrating the interpretation of well data and seismic reflection profiles available in the study area (Fig. 13) made available by the VIDEPI (2009) project (http://www.videpi.com). This seismic reflection dataset is represented by profiles belonging to the so-called "Zone B" plus other commercial profiles.

In the central Adriatic off-shore, the seismic reflection profiles, originally available as paper copies, have been transformed in digital segy files. The integrated interpretation of both seismic and well data has been carried out using dedicated software (Kingdom developed by Seismic Micro-Technology, Inc.). The seismic profiles have been interpreted to map the main seismic horizons (base of Quaternary, top of Messinian, top of Scaglia Calcarea (Middle Eocene), top of Marne a Fucoidi (Albian) and to define the geometry and the phases of tectonic activity of the recognized thrusts.

The resulting positions of the main thrusts, mapped at the top Scaglia Calcarea Fm horizon (i.e., Top Middle Eocene), are shown in Fig. 13.

On some seismic lines clear evidence of deformations affecting also the shallower section of the Quaternary units has been recognized (e.g., Fig. 13). These deformations can be related to the tectonic activity of the underlying thrusts. The thrust recognized in the western segment of seismic profile BR-232-03 (Fig. 13) is interpreted as a splay of another major thrust, located further west, which is responsible for the structural uplift of the Meso-Cenozoic sedimentary units outcropping in the Ancona promontory.

Although the documented shortening could have been accommodated by aseismic slip along the thrust surface, a link of this structure with the Composite Seismogenic Source ITCS008—Conero onshore proposed by DISS Working Group (2009)—is tentatively proposed. This source could be framed in the context of the known belt of active and seismogenic thrust-related folds recognized all along the northern Marche coastal belt, consistently with the occurrence of several historical and instrumental earthquakes and with the analysis of geomorphic features (e.g., Vannoli et al. 2004; Basili et al. 2008).

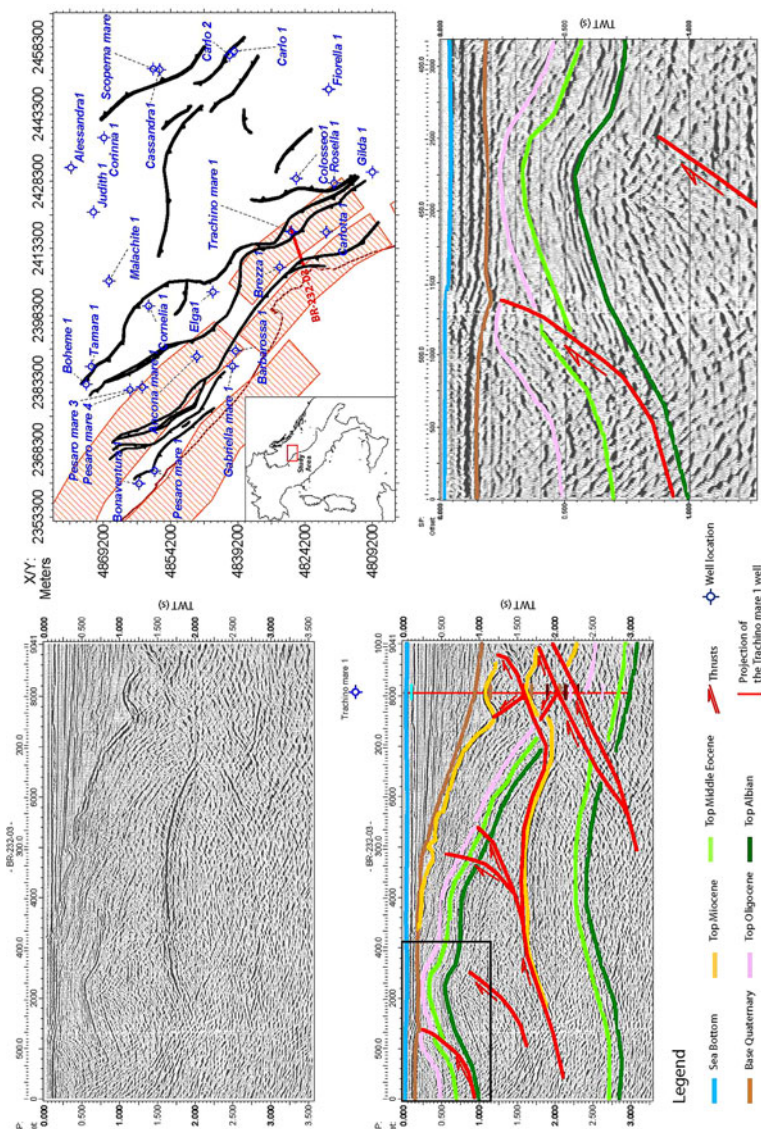

Fig. 13 *Upper right* map of the main thrusts (at top Scaglia Calcarea Fm) in the central Adriatic off-shore. Orange polygons are the composite seismogenic sources according to DISS Working Group (2009). Map projection is a standard Gauss-Boaga east zone. *Upper left* uninterpreted seismic reflection profile BR-232-03, location in the map above. *Lower right* interpreted section (main thrusts are in *red*). *Lower right* detail of the south-western portion of seismic profile BR-232-03 showing the deformation of the Quaternary sedimentary unit due to the underlying thrust fault. This thrust may be considered a splay of another major thrust located further west, which is responsible for the structural uplift of the Ancona promontory

In our tectonic interpretation of the central-northern Adriatic domain, the lack of contractional deformations in middle Pleistocene to recent deposits in the adjacent Adriatic offshore area, pointed out by some authors (e.g., Di Bucci and Mazzoli 2002), can be easily reconciled with the discussed evidence of tectonic activity (based on seismic reflection, geomorphological and seismological data) by observing that the belt affected by Late Quaternary to recent contractional deformations is located in a more internal position with respect to the position reached by the Apennine thrust front in Early Pleistocene times (e.g., Scrocca et al. 2007). The above reconstruction documents an early forward propagation of the thrust along an efficient detachment followed by a shift of the tectonic activity toward inner portion of the wedge. This tectonic behavior is coherent with the mechanics of accretionary wedge (e.g., Dahlen 1990; Boyer 1995; and references therein) and could be related to an increase of the dip of the regional monocline.

4 GPS data and strain rate field

The largest GPS time span covers an interval of 11 years (1998–2008). Nevertheless, most of the data come from the recent RING network (http://ring.gm.ingv.it) settled in Italy in the past 5 years by INGV. The GPS data processing follows basically the procedure proposed in Devoti et al. (2008).

We have analyzed the GPS observations at 30-s sampling rates in the framework of the processing of all the Italian permanent stations. Data were processed with the Bernese Processing Engine (BPE) of the Bernese software, version 5.0 (Beutler et al. 2007) based on the double difference observables. We have estimated each daily cluster in a loosely constrained reference frame, imposing a priori uncertainties of 10 m to obtain the so–called loosely constrained solution. The daily loosely constrained cluster solutions are then merged into global daily loosely constrained solutions of the whole network applying the classical least squares approach (Devoti et al. 2008). The daily combined network solutions are then rigidly transformed into the ITRF2005 frame (Altamimi et al. 2007), estimating translations and scale parameters.

The velocity field is estimated from the ITRF2005 time series of the daily coordinates, with the complete covariance matrix, simultaneously estimating site velocities, annual signals and offsets at epochs of instrumental changes, as in Devoti et al. (2008) and in Riguzzi et al. (2009). We have scaled the formal errors of the GPS rates using the mean scale factors estimated for each velocity component, as in Devoti et al. (2008), according to the approach developed in Williams (2003). GPS site positions and velocities with respect to the Eurasian fixed reference frame, defined in Devoti et al. (2008), with their re-scaled uncertainties are reported in Table 1 and Fig. 14. We have considered the GPS velocities separated in three clusters, accounting for the main tectonic domains (Fig. 14): the NE Alpine area, the NE Apennines-Po plain and the central-northern Apennines near the Umbria-Marche, and the offshore front areas. We have selected three different sections (a)–(c) crossing the fronts of deformations in the aforementioned areas. Figure 15 shows the GPS velocities projected along each section. We have considered velocities of all the sites located within 40 km in section (a) and 50 km in sections (b) and (c). The projected velocities are drawn versus the projected distance (in km) of each site from the southernmost point of each section. The dashed lines represent the position of the Alpine front along the section (a) and the Apennines one along the sections (b) and (c), respectively. Each section shows active shortening with an average linear trend in (a) and (b) at a mean

Table 1 GPS site positions, longitude and latitude are in degrees. East (E) and North (N) velocity components and their associated rescaled uncertainties (±E and ±N) are in units of mm/year. *Corr* correlation between the East and North velocity components, and Δt is the time span in units of year

Site	Longitude (°E)	Lattitude (°N)	E (mm/year)	N (mm/year)	±E (mm/year)	±N (mm/year)	Corr	Δ*t* (year)
Cluster 1								
ACOM	13.515	46.548	0.24	0.29	0.07	0.08	−0.03	5.5
AFAL	12.175	46.527	0.04	0.20	0.09	0.10	0.02	5.5
AMPE	12.799	46.415	0.03	0.32	0.10	0.11	−0.04	3.5
BRBZ	11.941	46.797	0.25	0.38	0.39	0.48	−0.01	3.5
CANV	12.435	46.008	0.06	0.79	0.09	0.10	−0.11	4.6
CAVA	12.583	45.479	0.15	2.20	0.10	0.08	−0.02	7.5
GSR1	14.544	46.048	0.07	1.91	0.14	0.17	−0.03	7.9
MDEA	13.436	45.925	−0.39	2.11	0.09	0.10	−0.09	6.0
MOGG	13.198	46.407	−0.08	1.06	0.07	0.09	0.02	5.5
MPRA	12.988	46.241	0.15	1.66	0.11	0.13	−0.07	6.5
PALM	13.308	45.905	0.02	2.04	0.07	0.08	−0.02	3.2
PORD	12.661	45.957	−0.29	1.16	0.19	0.23	0.00	4.2
TRIE	13.764	45.710	−0.43	2.00	0.07	0.09	−0.01	6.0
UDIN	13.253	46.037	−0.17	1.99	0.26	0.31	−0.01	4.0
VENE	12.332	45.437	0.32	1.42	0.11	0.14	−0.02	9.5
VLCH	13.851	46.607	1.05	0.77	0.07	0.08	−0.01	8.0
VLKM	14.626	46.661	1.00	0.68	0.10	0.12	−0.02	7.0
Cluster 2								
ASIA	11.525	45.866	−1.01	0.60	0.18	0.20	0.02	5.0
BOLG	11.357	44.500	−0.24	3.60	0.12	0.14	−0.00	4.3
CREA	9.685	45.354	0.42	0.42	0.35	0.41	−0.03	2.0
CREM	10.002	45.147	0.68	1.51	0.35	0.41	−0.02	2.0
FDOS	11.724	46.304	−0.55	−0.12	0.32	0.40	−0.01	2.3
MAGA	10.629	45.775	−0.94	0.24	0.24	0.28	−0.02	2.0
MODE	10.949	44.629	−0.38	3.51	0.24	0.28	−0.02	2.8
MSEL	11.646	44.520	1.31	2.52	0.17	0.37	0.00	4.3
PADO	11.896	45.411	0.24	1.05	0.08	0.09	−0.02	7.0
PARM	10.312	44.765	0.58	2.04	0.23	0.27	−0.02	3.2
ROVE	11.042	45.894	−0.81	0.16	0.48	0.54	−0.09	2.9
ROVI	11.783	45.087	−0.44	1.73	0.23	0.27	−0.01	4.1
SBPO	10.920	45.051	−0.37	1.12	0.21	0.25	−0.02	3.6
TEOL	11.677	45.343	−0.15	1.81	0.14	0.16	−0.03	4.7
UNFE	11.599	44.833	0.12	2.17	0.12	0.14	−0.07	6.7
VENE	12.332	45.437	0.32	1.42	0.11	0.14	−0.02	9.5
Cluster 3								
BRAS	11.113	44.122	0.78	1.38	0.04	0.05	−0.03	8.6
GUIE	12.565	43.352	0.88	2.52	0.39	0.45	0.01	2.0
IEMO	12.053	43.592	−0.38	1.69	0.25	0.29	−0.03	2.5
ITFA	12.926	43.344	0.45	2.64	0.16	0.18	−0.01	3.5
ITRN	12.582	44.048	0.34	1.32	0.70	0.82	−0.01	2.0

Table 1 continued

Site	Longitude (°E)	Lattitude (°N)	E (mm/year)	N (mm/year)	±E (mm/year)	±N (mm/year)	Corr	Δ*t* (year)
MEDI	11.647	44.520	1.22	1.70	0.06	0.06	−0.02	11.0
MOIE	13.124	43.503	1.12	3.01	0.16	0.18	−0.03	3.9
MVAL	12.407	43.382	1.44	2.36	0.40	0.46	−0.03	2.5
PES1	12.893	43.893	0.68	3.08	0.71	0.80	−0.01	1.9
PRAT	11.099	43.885	0.80	1.93	0.06	0.14	−0.01	9.9
RSMN	12.451	43.934	1.24	4.25	0.13	0.14	−0.02	4.1
UNUB	12.640	43.701	1.30	3.03	0.31	0.36	−0.02	2.0

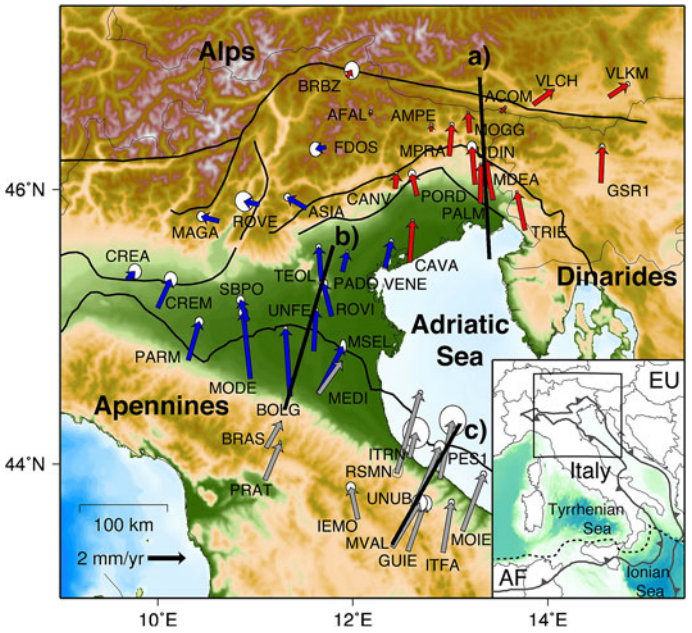

Fig. 14 GPS velocities relative to Eurasia with rescaled error ellipses, in the northern Adriatic plate realm, where three subduction zones interacts (Apennines, Alps and Dinarides). Velocities are divided into three clusters (*red* 1, *blue* 2, and *gray* 3) to estimate local strain rates. Section (*a*), (*b*), and (*c*) are those related to Fig. 16. *EU* Europe, *AF* Africa

rate of about 2 mm/year, whereas section (c) shows a steep gradient even if with a larger uncertainty.

Subsequently, we estimate the strain rate field solving the two–dimensional velocity gradient tensor equations, with an inverse procedure, based on the standard least squares approach.

We use a regularly spaced gridded interpolation method, based on the distance-weighted approach (Shen et al. 1996; Allmendinger et al. 2007; Cardozo and Allmendinger 2009). We define a regular grid (5 × 5 km) estimating the strain rate principal axes at the center of each cell, using all the GPS velocities pertaining to each cluster. The velocity of

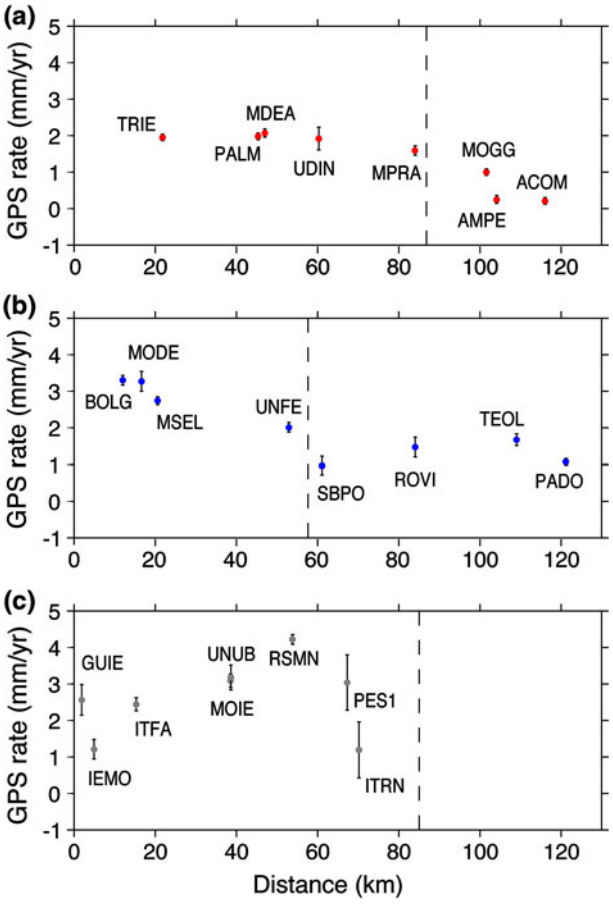

Fig. 15 GPS velocities projected on the sections (**a**), (**b**), (**c**) of the Fig. 14. *Dashed lines* represent the position of the Alpine front along the section (**a**) and the Apennines one along the sections (**b**) and (**c**), respectively

each station is weighted by the factor $W = \exp(-d^2/2\alpha^2)$, where d is the distance between each GPS site and the center of the cell, and α (22 km) is the damping parameter defining how the contribution of each station decays with distance from the cell center. The pattern of the strain rate principal axes (Fig. 16) shows that most of shortening directions tend to be perpendicular to the thrust belt fronts, reaching 82 ± 11 nstrain/year in cluster 1 (Eastern Veneto, Friuli, Southern Austria), 44 ± 8 nstrain/year in cluster 2 (Western Veneto, Lombardy, Emilia-Romagna) and with lower values offshore, in cluster 3 (Marche), where the GPS velocities are not able to constrain with good accuracy the deformation rate. The extension rate axes reach the maximum value of 45 ± 19 nstrain/year in cluster 1; minor rates are 35 ± 15 nstrain/year in cluster 2 and 56 ± 18 nstrain/year in cluster 3. Figure 17 shows comparisons between compression and extension for clusters 1, 2, and 3, respectively, estimated on a regularly spaced grid 5×5 km. Detailed surface plots show a shortening of $\sim$20 nstrain/year for cluster 1 and cluster 2 with large values in the northwestern side of the Alps and in the Po Plain around the Apennines front, respectively. On average, extension is also $\sim$20 nstrain/year for cluster 1 and cluster 2,

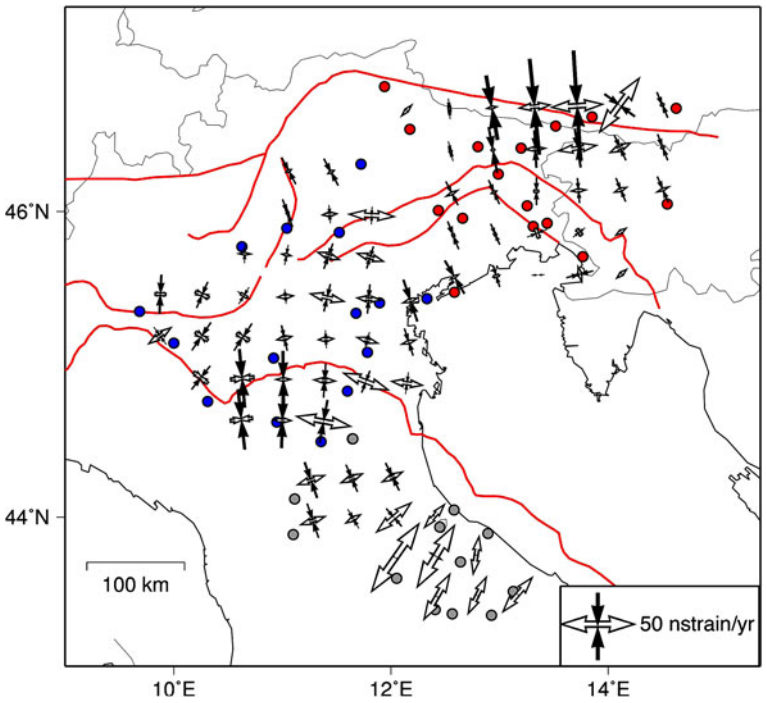

Fig. 16 Principal axes of strain rates from GPS velocities in the northern Adriatic plate area (Northern Apennines and Southern Alps), estimated on a regularly spaced grid (5 × 5 km), here plotted every 30 km. *Black* and *white arrows* represent shortening and extension rate principal axes. *Red*, *blue*, and *gray dots* are the GPS stations of the cluster 1, cluster 2, and cluster 3, respectively. On average, the estimated strain rates are within 20 nstrain/year, with higher values of compression in the northeastern side of the Alps and in the Po Plain, whereas there are high values of extension in the inner Apennines. Note the smaller strain rate along the Ferrara salient, and in the Venetian foothills, which may indicate tectonic loading

except for higher values in the northwestern side of the Alps and around the Ferrara salient for cluster 1 and cluster 2, respectively. Cluster 3 shows on average high values of compression and the largest of extension (∼60 nstrain/year) in the Umbria-Marche area where the seismic sequence of 1997 took place. It is evident that moving along the active front of the orogens surrounding the Adriatic plate, the areas of low strain rate are those where there is the largest tectonic loading, i.e., they are more prone to generate earthquakes. Other areas of larger strain rate indicate aseismic creep, possibly the record of the steady-state ductile deformation at depth.

5 Vertical motion

Long-term (1 Ma) subsidence rates, computed by measuring the synsedimentary tilting of the regional monocline all around the Apennines, are about 1 mm/year (Fig. 8; Carminati et al. 2003). We also crosschecked long-term subsidence rates with those computed for the past 125 kyr (using the Marine Isotope Stage 5.5, Tyrrhenian layer, Fig. 10; Antonioli et al. 2009). The upper Pleistocene Tyrrhenian sediments of the northern Adriatic coast have been cored to measure their depth (Antonioli et al. 2009). This layer shows an

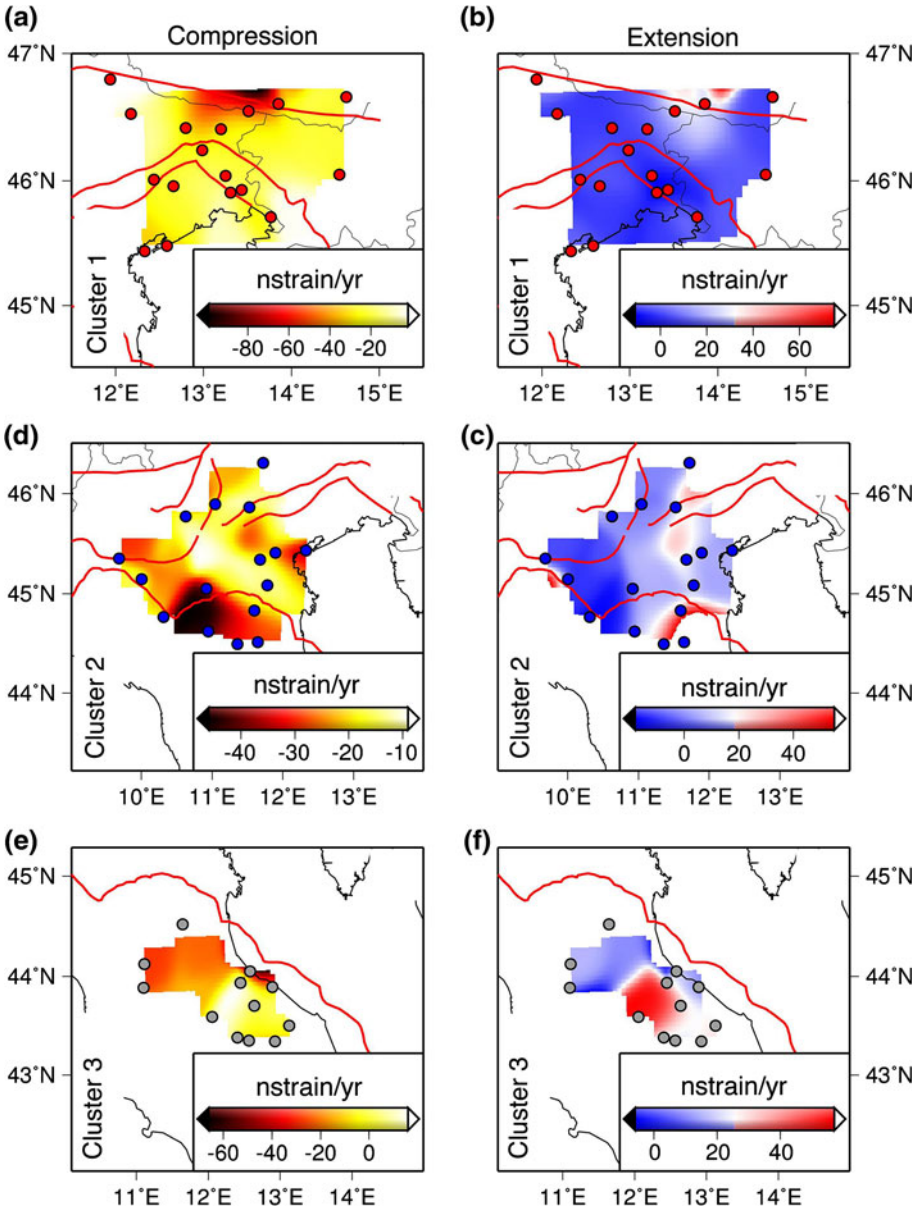

Fig. 17 Comparison between compression and extension for cluster 1, 2, and 3, respectively, estimated on a regularly spaced grid 5 × 5 km. Detailed surface plots show a shortening of ∼20 nstrain/year for cluster 1 (**a**) and cluster 2 (**c**) with high values in the northwestern side of the Alps, and in the Po Plain around the Apennines front, respectively. Extension is also ∼20 nstrain/year for cluster 1 (**b**) and cluster 2 (**d**) except for higher values in the northwestern side of the Alps and around the Ferrara salient for cluster 1 and cluster 2, respectively. Cluster 3 shows on average high values of compression (**e**) and the largest of extension (**f**) (∼60 nstrain/year)

increasing depth moving from northeast to southwest, consistently with the long-term subsidence rates.

Considering GPS observations, vertical rates from GPS should be carefully considered, due to the intrinsic lower capability of GPS to detect vertical motion with respect to the horizontal one. In Table 2 we show all the GPS sites analyzed in this paper, their vertical rates, the re-scaled uncertainties, and the time length of the observations. Subsidence rates reach the maximum value 11.4 ± 1.1 mm/year near Modena (MODE) and averagely decrease toward NE (Fig. 18, map and insets). Figure 18 shows an interpolated surface plot of the vertical GPS rates reported in Table 2, applying the methods proposed by Smith and Wessel (1990). The map highlight an asymmetric subsidence in the Apennines foreland basin, being faster toward the depocenter to the southwest (Fig. 18), although faster than the rates inferred by the geological indicators.

Our GPS vertical rates are comparable with those estimated by Baldi et al. (2009) both in terms of magnitudes and uncertainties (Table 2; Baldi et al. 2009). With respect to other techniques (InSAR, leveling) GPS rates appear systematically higher, especially when the time series are not very long, as underlined both in Baldi et al. (2009) for the same area and in Riguzzi et al. (2009) in the Colli Albani area.

Subsidence rates may reflect both anthropogenic effects (water extraction), and/or to the larger compaction effect on the shallow sediments (e.g., Carminati and Martinelli 2002). However, the pattern showed in Fig. 18 claims for a regional influence of the Apennines subduction on the sea-level rise and asymmetric subsidence in the northern Adriatic realm, an area presently undergoing the combined effects of the Dinarides and Alpine subduction as well.

6 Discussion and conclusions

The northern Adriatic plate boundaries are deformed by the three belts, i.e., Apennines, Alps, and Dinarides. The Adriatic plate represents the lower plate of the Apennines and Dinarides, whereas it is the upper plate for the Alps. The western Adriatic plate boundary is deformed by the Apennines which have no converging and overriding upper plate, and the accretionary prism is mostly made of the lower plate rocks, apart the inherited Alpine nappe stacking in the inner core of the Apennines. In the Southern Alps, the deformation involves the upper plate alone (Adriatic plate northern margin) of the Alpine subduction zone, whereas the frontal Dinarides are the thrust belt affecting only the lower plate (Adriatic plate eastern margin) along the Dinarides subduction system.

The faster subsidence of the Pleistocene sediments, including Holocene and Tyrrhenian, along the western side of the northern Adriatic area (Fig. 10) confirms a link between subsidence and the SW-ward tilting of the foreland regional monocline of the Apennines, associated with the retreat of the subduction hinge. The hinge of the northern Apennines slab is still moving toward the NE, away from the upper plate (Devoti et al. 2008), inducing subsidence in the downgoing lithosphere that decreases moving toward the foreland (Fig. 11). The northern Adriatic lithosphere is also suffering the effects of the subductions of the Alps and the Dinarides. The asymmetry of Pleistocene subsidence, however, indicates that the Apennines have the most relevant role in shaping the vertical rates in the northern Adriatic realm, tilting both the Alps and the Dinarides orogens toward the foreland. GPS data suggest that southward tilting of the front of the Southern Alps occurs in their central and western parts, whereas the front in the Friuli area to the east is

Table 2 GPS site positions, longitude and latitude are in degrees. Vertical GPS velocity component (Up) and its associated rescaled uncertainty (±Up) is in units of mm/year. Δt is the time span in units of year

Site	Longitude (°E)	Latitude (°N)	Up (mm/year)	±Up (mm/year)	Δt (year)
ACOM	13.515	46.548	1.6	0.3	5.5
AFAL	12.175	46.527	2.5	0.8	5.5
AMPE	12.799	46.415	1.4	0.4	3.5
AREZ	11.875	43.464	4.0	1.6	1.9
ASIA	11.525	45.866	−0.6	0.8	5.0
BOLG	11.357	44.500	−2.5	0.5	4.3
BORM	10.364	46.468	1.0	2.2	2.0
BRAS	11.113	44.122	1.2	0.1	8.6
BRBZ	11.941	46.797	3.0	1.8	3.5
BREA	10.233	45.565	2.0	1.9	2.0
BRIX	10.233	45.565	1.3	0.5	4.5
BZRG	11.337	46.499	1.5	0.3	11.0
CAIE	12.248	43.467	2.4	1.1	4.8
CALA	11.164	43.868	0.7	1.7	2.0
CANV	12.435	46.008	1.3	0.4	4.6
CARP	10.427	45.368	−0.3	1.9	1.9
CASN	10.301	45.471	0.4	1.9	2.0
CAVA	12.583	45.479	−2.0	0.4	7.5
CITT	12.248	43.467	0.4	1.7	2.0
CREA	9.685	45.354	−1.1	1.4	2.0
CREM	10.002	45.147	−0.2	1.4	2.0
CRMI	10.980	43.796	0.9	1.5	2.3
FDOS	11.724	46.304	−0.4	1.5	2.3
GAZZ	9.829	45.794	−1.6	2.1	2.0
GROG	9.892	43.426	2.0	1.0	3.4
GSR1	14.544	46.048	0.0	0.6	7.9
GUIE	12.565	43.352	5.9	1.8	2.0
IEMO	12.053	43.592	6.9	1.1	2.5
ITFA	12.926	43.344	3.7	0.7	3.5
MDEA	13.436	45.925	−0.1	0.4	6.0
MEDI	11.647	44.520	−0.7	0.2	11.0
MOCA	11.143	46.098	0.1	1.4	2.1
MODE	10.949	44.629	−11.4	1.1	2.8
MOGG	13.198	46.407	1.3	0.3	5.5
MOIE	13.124	43.503	−0.1	1.3	3.9
MPRA	12.988	46.241	0.8	0.5	6.5
MSEL	11.647	44.520	−2.1	0.7	4.3
MVAL	12.407	43.382	1.7	1.8	2.5
PADO	11.896	45.411	0.0	0.2	7.0
PALM	13.308	45.905	1.1	0.3	3.2
PARM	10.312	44.765	0.5	1.0	3.2
PORD	12.661	45.957	−0.1	0.9	4.2

Table 2 continued

Site	Longitude (°E)	Latitude (°N)	Up (mm/year)	±Up (mm/year)	Δt (year)
PRAT	11.099	43.886	0.0	0.2	9.9
ROVE	11.042	45.894	−2.8	2.1	2.9
ROVI	11.783	45.087	−3.1	1.1	4.1
RSMN	12.451	43.934	2.3	0.6	4.1
SALO	10.524	45.618	−2.7	2.3	3.2
SBPO	10.920	45.051	1.3	0.9	3.6
SGIP	11.183	44.636	−4.8	1.1	3.5
TEOL	11.677	45.343	0.5	0.6	4.7
TRIE	13.764	45.710	0.5	0.3	6.0
UDIN	13.253	46.037	0.5	1.2	4.2
UNFE	11.599	44.833	−1.1	0.5	6.7
UNUB	12.640	43.701	−0.2	1.3	2.0
UPAD	11.878	45.407	0.0	0.2	4.0
VENE	12.332	45.437	−0.7	0.4	9.5
VLCH	13.851	46.607	1.1	0.3	8.0
VLKM	14.626	46.661	0.7	0.5	7.0
VOLT	11.911	45.385	−0.4	0.3	7.3
ZOUF	12.974	46.557	3.2	0.5	6.5

uplifting. This different behavior is probably due to the increasing distance (from west to east) of the front of the Alps with respect to the Apennines subduction hinge.

The effects of four independent Neogene to present subduction zones coexist in northeast Italy:

1. The dominant one is the Alpine subduction, where Europe subducted the Adriatic plate closing the pre-existing intervening ocean. The Southern Alps are the retrobelt of the related Alpine orogen.
2. The Alpine belt overlapped/interfered with the frontal thrust belt of the Dinarides, where the Adriatic plate rather subducted the Eurasia plate.
3. Moving north-eastward, normal faults of the Pannonian backarc basin of the Carpathians subduction crosscut the Northern Dinarides and part of the Eastern Alps.
4. The hinge retreat of the Apennines subduction determines asymmetric subsidence of entire northern Italy and of the Adriatic basin.

This indicates that separate geodynamic settings can coexist in a given area, and the related stress fields may interfere or overlap.

Referring to the previous points:

1. The Transalp section (Castellarin et al. 2006) confirmed the double vergent asymmetric structure of the Alps (Dal Piaz et al. 2003). The Southern Alps are notoriously bounded to the north by the right-lateral transpressive Insubric Lineament, and in this sector the vergence of the thrusts is toward the subduction hangingwall, i.e., the Adriatic plate. During pre-Eocene collision stages, subduction zones exhibit well-developed retrobelts, such as the SubAndean belt, or the Rocky Mountains in the Southern and Northern America Cordilleras, respectively. These analogs would suggest that, in the retrobelt of the Alps, shortening could have started since the early

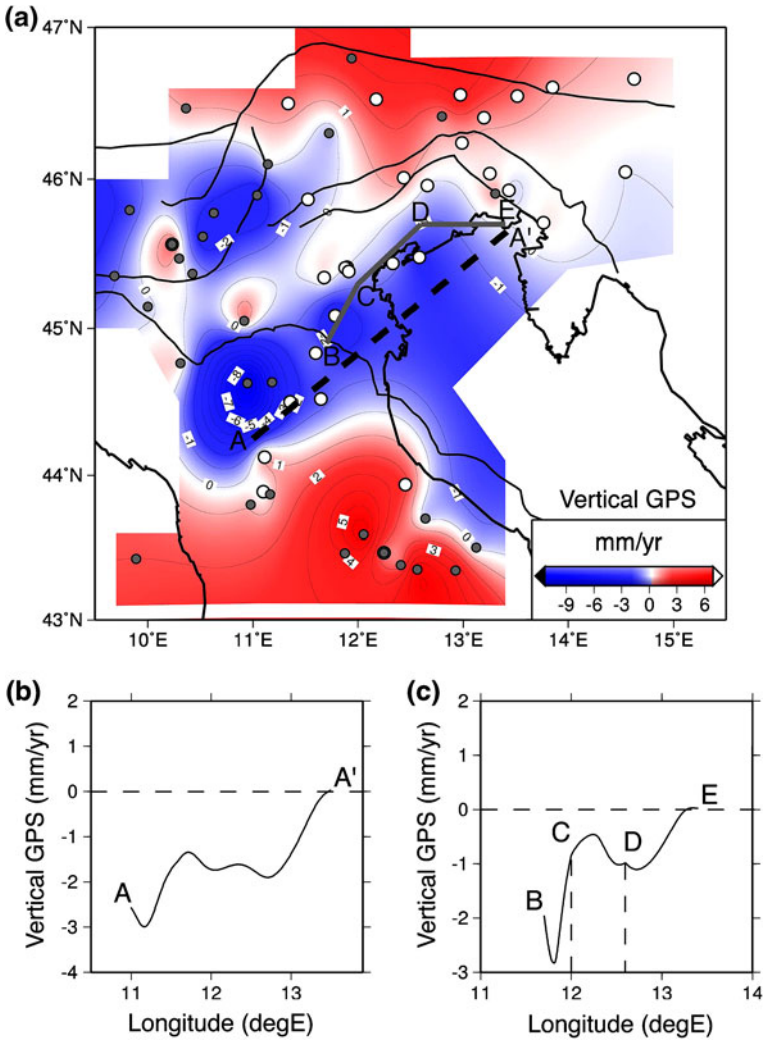

Fig. 18 **a** Interpolated surface of the vertical GPS velocity component obtained from data of cluster 1, 2, 3, and additional GPS stations reported in Table 2. *White* and *gray dots* represent sites with time span >4 years and <4 years, respectively. Vertical GPS rates of the western northern Adriatic show present-day faster subsidence (>1 mm/year). Profiles **b** and **c** in the overlying map. The trend of subsidence can be attributed to the northeastward migration of the Apennines subduction hinge

stages of the subduction. The Transalp section does not show N–S extension in the Alps, excluding significant orogenic collapse as frequently proposed for the Alps and orogens in general. The E–W extension in the Alps as the one described along the Brenner Line at the western margin of the Tauern Window (e.g., Ratschbacher et al. 1989; Selverstone 2005) and at its eastern margin (Genser and Neubauer 1989) can be interpreted as upper crustal stretching related to the culmination of the Tauern antiform. The axial culmination of the anticline formed contemporaneously to the Brenner Line (which offset is concentrated at the western margin of the Tauern anticline indicating a common genesis). Line balancing of any stratigraphic reference

layer kinematically requires an along axis elongation of the growing belt due to the antiform culmination. Therefore, the longitudinal extension and uplift can be explained by the compression perpendicular to the belt.

2. The Dinarides and the Alps merged to generate a single belt in the Eastern Alps, but they are still related to separated geodynamic processes, i.e., two independent subduction zones (Fig. 1).
3. The Carpathians subduction probably followed the same geodynamic scenario of the Apennines, which first developed along the retrobelt of the Alps, where, in the foreland (i.e., to the east), there was oceanic or thinned continental lithosphere. This evolution bears similarities with the evolution of the W-directed subduction zones of the Barbados and the Sandwich arcs in the Atlantic ocean (Doglioni et al. 1999). According to this interpretation, the Carpathians developed along the retrobelt of the northern Dinarides, such as the Balkans, where oceanic or thinned continental lithosphere of the Dacide basin was located to the east of the retrobelt. The consumption of this basin accompanied the eastward retreat of the subduction to the present position in Vrancea. This implies that elements of both Alps and Dinarides, stretched and scattered, are buried in the Pannonian basin.
4. Since the Paleogene, the Venetian, and Friuli plains underwent subsidence due to the load of the Alpine and Dinarides thrust sheets, forming two related and anastomosed foredeeps. However, the thinning of the Pliocene-Quaternary sediments (Merlini et al. 2002), and the dip decrease of the regional monocline moving away from the Apennines front (Mariotti and Doglioni 2000; Carminati et al. 2003), they all indicate active subsidence all around this belt. The Apennines foreland subsidence affected most of the Alps and external Dinarides. The long-term subsidence of Venice and other cities along the coast was determined by the retreat of the subduction hinge of the Adriatic plate dipping underneath the Apennines (Fig. 9). The flexure of the subduction hinge affects, to the NE, areas more than 250 km far from the Apennines front (Fig. 12). The Apennines slab is continental and has no negative buoyancy relative to the underlying mantle. Therefore, the slab rollback here cannot be ascribed to slab pull. Alternatively, the "eastward" relative mantle flow implicit in the "westward" drift of the lithosphere could explain the forced sinking of the slab.

Northeast Italy is usually interpreted as an area affected by N–S compression due to the African-Adriatic indenter. However, this comes from a misleading kinematic approach, where local stress field is assumed to be an indicator of plate motion. The stress field rotates along oblique plate margins, and the WNW-ward motion of the Adriatic plate relative to Europe can generate right-lateral transpression and consequent NW–SE to N–S compression along the central-eastern Alps. Moreover, the Adriatic plate and Europe, in the no-net-rotation (ITRF) reference frame (Heflin et al. 2009), are both moving north-eastward, and not in a north–south direction. European and Adriatic plates have different north–south component, but they move between 45E and 52E absolute directions. The variable azimuth of the stress field all around the Adriatic plate is the composite direction of relative plate motions, plus the structural undulations generated by the anistropies in the involved lithospheres. Therefore, they may be strongly deviated with respect to the direction of plates in the ITRF or even in the HSRF (hotspot reference frame).

The relatively high topography of the Alps is consistent with crustal scale thrusting (Doglioni 1987, 1992b; Pfiffner et al. 1997; Schonborn 1999; Kummerow et al. 2004). In spite of elevated topography and more than 50-km-thick continental crust (Kissling 1993), the Alps, both in the frontal belt to the north and in the conjugate retrobelt to the south,

present low dip of the foreland regional monocline (3–5°), typical of "E"-directed subduction zones, in contrast with the Apennines, due to a "W"-directed subduction zone, associated with low topography and regional monocline as steep as 20° (Mariotti and Doglioni 2000). As a general rule, salients of the thrust belt in the Southern Alps and adjacent orogens occur along inherited Mesozoic grabens characterized by thicker sequences. Therefore, several transfer zones occur, related to pre-existing structural and stratigraphic lateral variations of the passive margin architecture (e.g., platform to basin transition, N–S trending horsts and grabens). Moving along strike from the Transalp section, thrust belt transfers occur mainly through lateral variation of the ramp distance. Of course, these lateral changes of the dip of the regional monocline induced by rheological differences within the sedimentary pile are associated with crustal or lithospheric scale rheological changes. Bertotti et al. (1998) have proposed a continuous increase through time (from the Paleogene onwards) of the dip of the regional monocline in the foredeep basin of the Southern Alps. They related such changes to a decrease (from 20 km to less than 5 km) of the elastic plate thickness, associated with a weakening of the flexed subducting plate.

Apart from local regional details, the main conclusions based on seismic reflection profiles and space geodesy data are that the three belts around the northern Adriatic plate are still converging and seismically active. The vertical movements, positive in the axial portions of the belts to indicate their uplift, show a strong asymmetric signature, being subsidence faster along the Apennines margin of the related foreland basin. This indicates an active slab retreat of the Apennines subduction zone. Finally, as a general consideration, the coexistence of different geodynamic mechanisms acting on the northern Adriatic plate implies that plate boundaries may overlap and interact at the same time in the same area. This supports the notion that plate boundaries are passive features, e.g., the slab pull is possibly not the driving force of plate motion (Doglioni et al. 2007).

Acknowledgments Thanks to the two constructive reviewers and Giorgio Vittorio Dal Piaz who provided helpful suggestions. We are also grateful to the Seismic Micro-Technology, Inc. for making available the Kingdom software. Research supported by TopoEurope, Topo-4D project, CNR. Some of the figures were made with the Generic Mapping Tools of Wessel and Smith (1995).

References

Allmendinger RW, Reilinger R, Loveless J (2007) Strain and rotation rate from GPS in Tibet, Anatolia, and the Altiplano. Tectonics 26. doi:10.1029/2006TC002030

Altamimi Z, Collilieux X, Legrand J, Garayt B, Boucher C (2007) ITRF2005: a new release of the International Terrestrial Reference Frame based on time series of station positions and Earth Orientation Parameters. J Geophys Res 112. doi:10.1029/2007JB004949

Antonioli F, Ferranti L, Fontana A, Amorosi AM, Bondesan A, Braitenberg C, Dutton A, Fontolan G, Furlani S, Lambeck K, Mastronuzzi G, Monaco C, Spada G, Stocchi P (2009) Holocene relative sea-level changes and vertical movements along the Italian coastline. J Quat Int 231:37–51

Argand E (1924) La tectonique de l'Asie. In: Proc Int Geol Congr, vol XIII, pp 171–372

Argnani A, Artoni A, Ori G, Roveri M (1991) L'avanfossa centro-adriatica: stili strutturali e sedimentazione. Studi Geol Camerti 1991/1:371–381

Baldi P, Casula C, Cenni N, Loddo F, Pesci A (2009) GPS-based monitoring of land subsidence in the Po Plain (Northern Italy). Earth Planet Sci Lett 288:204–212

Basili R, Valensise G, Vannoli P, Burrato P, Fracassi U, Mariano S, Tiberti M, Boschi E (2008) The database of individual Seismogenic Sources (DISS), version 3: summarizing 20 years of research on Italy's earthquake geology. Tectonophysics 453:20–43

Benedetti LC, Tapponnier P, Gaudemer Y, Manighetti I, Van der Woerd J (2003) Geomorphic evidence for an emergent active thrust along the edge of the Po Plain: the Broni-Stradella fault. J Geophys Res 108(B5):2238. doi:10.1029/2001JB001546

Bertotti G, Picotti V, Bernoulli D, Castellarin A (1993) From rifting to drifting: tectonic evolution of the Southalpine upper crust from the Triassic to the Early Cretaceous. Sediment Geol 86(1-2):53–76
Bertotti G, ter Voorde M, Cloetingh S, Picotti V (1997) Thermo-mechanical evolution of the South Alpine rifted margin (North Italy): constraints on the strength of passive continental margins. Earth Planet Sci Lett 146:181–193
Bertotti G, Picotti V, Cloetingh S (1998) Lithospheric weakening during "retro-foreland" basin formation: tectonic evolution of the central South Alpine foredeep. Tectonics 17(1):131–142
Beutler et al (2007) In: Dach R, Hugentobler U, Fridez P, Meindl M (eds) Bernese GPS software. Astronomical Institute, University of Bern
Bigi G, Castellarin A, Coli M, Dal Piaz GV, Sartori M, Scandone P, Vai GB (1990) Structural model of Italy. sELCA, Florence
Boyer SE (1995) Sedimentary basin taper as a factor controlling the geometry and advance of thrust belt. Am J Sci 295:1220–1254
Bressan G, Snidarcig A, Venturini C (1998) Present state of tectonic stress of the Friuli area (eastem Southern Alps). Tectonophysics 292:211–227
Cardozo N, Allmendinger RW (2009) SSPX: A program to compute strain from displacement/velocity data. Comput Geosci 35:1343–1357
Carminati E, Martinelli G (2002) Subsidence rates in the Po plain (Northern Italy): the relative impact of Natural and Anthropic causation. Eng Geol 66:241–255
Carminati E, Doglioni C, Scrocca D (2003) Apennines subduction-related subsidence of Venice. Geophys Res Lett 30. doi:10.1029/2003GL017001
Carminati E, Doglioni C, Scrocca D (2005) Magnitude and causes of long-term subsidence of the Po Plain and Venetian region. In: Fletcher CA, Spencer T, Mosto JD, Campostrini P (eds) Flooding and environmental challenges for venice and its lagoon: state of knowledge. Cambridge University Press
Carminati E, Cavazza D, Scrocca D, Fantoni R, Scotti P, Doglioni C (2010a) Thermal and tectonic evolution of the Southern Alps (Northern Italy) rifting: coupled organic matter maturity analysis and thermo-kinematic modelling. AAPG Bull 94(3):369–397. doi:10.1306/08240909069
Carminati E, Scrocca D, Doglioni C (2010b) Compaction-induced stress variations with depth in an active anticline: Northern Apennines, Italy. J Geophys Res 115:B02401. doi:10.1029/2009JB006395
Casero P, Rigamonti A, Iocca M (1990) Paleogeographic relationships durino cretaceous between the northern Adriatic area and the eastern Southern Alps. Mem Soc Geol It 45:807–814
Castellarin A, Cantelli L, Fesce AM, Mercier J, Picotti V, Pini GA, Prosser G, Selli L (1992) Alpine compressional tectonics in the Southern Alps. Relationships with the N-Apennines. Ann Tectonicae VI(1):62–94
Castellarin A, Nicolich R, Fantoni R, Cantelli L, Sella M, Selli L (2006) Structure of the lithosphere beneath the Eastern Alps (southern sector of the TRANSALP transect). Tectonophysics 414:259–282
Castello B, Selvaggi G, Chiarabba C, Amato A (2006) CSI Catalogo della sismicita italiana 1981–2002, version 1.1, INGV–CNT, Rome. http://csi.rm.ingv.it/
Catalano R, Doglioni C, Merlini S (2001) On the Mesozoic Ionian basin. Geophys J Int 144:49–64
Consiglio Nazionale delle Ricerche (1992) Structural model of Italy and gravity map, progetto Finalizzato Geodinamica. Quaderni de "La Ricerca Scientifica", 114, vol 3
D'Agostino N, Cheloni D, Mantenuto S, Selvaggi G, Michelini A, Zuliani D (2005) Interseismic strain accumulation in the eastern Southern Alps (NE Italy) and deformation at the eastern boundary of the Adria block observed by CGPS measurements. Geophys Res Lett 32. doi:10.1029/2006GL024266
Dahlen FA (1990) Critical taper model of fold and thrust belts and accretionary wedge. Earth Planet Sci Lett 19:55–99
Dal Piaz GV, Bistacchi A, Massironi M (2003) Geological outline of the Alps. Episodes 26:175–180
Devoti R, Riguzzi F, Cuffaro M, Doglioni C (2008) New GPS constraints on the kinematics of the Apennines subduction. Earth Planet Sci Lett 273:163–174
Di Bucci D, Mazzoli S (2002) Active tectonics of the Northern Apennines and Adria geodynamics: new data and a discussion. J Geodyn 34:687–707
Di Stefano R, Kissling E, Chiarabba C, Amato A, Giardini D (2009) Shallow subduction beneath Italy: Three-dimensional images of the Adriatic–European–Tyrrhenian lithosphere system based on high-quality P wave arrival times. J Geophys Res 114. doi:10.1029/2008JB005641
Doglioni C (1987) Tectonics of the Dolomites (Southern Alps, Northern Italy). J Struct Geol 9:181–193
Doglioni C (1992a) Relationships between Mesozoic extensional tectonics, stratigraphy and Alpine inversion in the Southern Alps. Eclog Geol Helv 85:105–126
Doglioni C (1992b) The Venetian Alps thrust belt. In: McClay K (ed) Thrust tectonics. Chapman amd Hall, pp 319–324

Doglioni C, Carminati E (2002) The effects of four subductions in NE Italy. Transalp conference. Mem Sci Geol 54:1–4
Doglioni C, Carminati E (2008) Structural styles and dolomites field trip. Mem Descrittive Carta Geol d'Italia 92:1–299
Doglioni C, Harabaglia P, Merlini S, Mongelli F, Peccerillo A, Piromallo C (1999) Orogens and slabs vs. their direction of subduction. Earth Sci Rev 45:167–208
Doglioni C, Carminati E, Cuffaro M, Scrocca D (2007) Subduction kinematics and dynamic constraints. Earth Sci Rev 83:125–175
Galadini F, Poli ME, Zanferrari A (2005) Seismogenic sources potentially responsible for earthquakes with $M > 6$ in the eastern Southern Alps (Thiene-Udine sector, NE Italy). Geophys J Int 160:1–24
Genser J, Neubauer F (1989) Low angle normal faults at the eastern margin of the Tauern window (Eastern Alps). Mitt Oesterr Geol Ges 81:233–243
DISS Working Group (2009) Database of individual seismogenic sources (diss), version 3.1.0: a compilation of potential sources for earthquakes larger than m 5.5 in italy and surrounding areas. ©INGV 2009—Istituto Nazionale di Geofisica e Vulcanologia—All rights reserved. http://diss.rm.ingv.it/diss/
Heflin et al (2009) GPS time series. Jet Propulsion Laboratory, California Institute of Technology. http://sideshow.jpl.nasa.gov/mbh/series.html
Kissling E (1993) Deep structure of the Alps; what do we really know? Phys Earth Planet Int 79:87–112
Kummerow J, Kind R, Onken O, Giese P, Ryberg T, Wylegalla K, Scherbaum F, TRANSALP Working Group (2004) A natural and controlled source seismic profile through the Eastern Alps: TRANSALP. Earth Planet Sci Lett 225:115–129
Mariotti G, Doglioni C (2000) The dip of the foreland monocline in the Alps and Apennines. Earth Planet Sci Lett 181:191–202
Merlini S, Doglioni C, Fantoni R, Ponton M (2002) Analisi strutturale lungo un profilo geologico tra la linea Fella–Sava e l'avampaese adriatico (Friuli Venezia Giulia—Italia). Mem Soc Geol It 57:293–300
Montone P, Mariucci MT, Pondrelli S, Amato A (2004) An improved stress map for Italy and surrounding regions (central Mediterranean). J Geophys Res 109. doi:10.1029/2003JB002703
Ori G, Roveri M, Vannoni F (1986) Plio-Pleistocene sedimentation in the Apenninic–Adriatic foredeep (Central Adriatic Sea, Italy). Spec Publ Int Ass Sediment 8:183–198
Panza GF, Raykova RB (2008) Structure and rheology of lithosphere in Italy and surrounding. Terra Nova 20:194–199
Panza GF, Mueller S, Calcagnile G, Knopoff L (1982) Delineation of the north central Italian upper mantle anomaly. Nature 296:238–239
Panza GF, Pontevivo A, Chimera G, Raykova R, Aoudia A (2003) The lithosphere–asthenosphere: Italy and surroundings. Episodes 26:169–174
Panza GF, Peccerillo A, Aoudia A, Farina B (2007) Geophysical and petrological modelling of the structure and composition of the crust and upper mantle in complex geodynamic settings: the Tyrrhenian Sea and surroundings. Earth Sci Rev 80:1–46
Pfiffner OA, Lehener P, Heizmann P, Mueller S, Steck A (1997) Results of NRP20-Deep structure of the Alps. Birkhäuser Verlag, Basel
Picotti V, Pazzaglia FJ (2008) A new active tectonic model for the construction of the Northern Apennines mountain front near Bologna (Italy). J Geophys Res 113:B08412. doi:10.1029/2007JB005307
Ratschbacher L, Frisch W, Neubauer F, Schmid SM, Neugebauer J (1989) Extension in compressional orogenic belts: the Eastern Alps. Geology 17:404–407
Riguzzi F, Pietrantonio G, Devoti R, Atzori S, Anzidei M (2009) Volcanic unrest of the Colli Albani (central Italy) detected by GPS monitoring test. Phys Earth Planet Int 177:79–87
Royden L (1993) The tectonic expression slab pull at continental convergent boundaries. Tectonics 12:303–325
Schonborn G (1999) Balancing cross sections with kinematic constraints: the Dolomites (northern Italy). Tectonics 18:527–545
Scrocca D (2006) Thrust front segmentation induced by differential slab retreat in the Apennines (Italy). Terra Nova 18:154–161
Scrocca D, Carminati E, Doglioni C, Marcantoni D (2007) Slab retreat and active shortening along the Central-Northern Apennines. In: Lacombe O, Lavй J, Roure F, Verges J (eds) Thrust belts and Foreland Basins: from fold kinematics to hydrocarbon systems. Frontier in Earth Sciences, Springer, pp 471–487
Selverstone J (2005) Are the Alps collapsing? Annu Rev Earth Planet Sci 33:113–132. doi: 10.1146/annurev.earth.33.092203.122535
Shen ZK, Jackson DD, Ge BX (1996) Crustal deformation across and beyond the Los Angeles basin from geodetic measurements. J Geophys Res 101:27957–27980

Slejko D, Neri G, Orozova I, Renner G, Wyss M (1999) Stress field in Friuli (NE Italy) from fault plane solutions of activity following the 1976 main shock. Bull Seismol Soc Am 89:4

Smith WHF, Wessel P (1990) Gridding with continuous curvature splines in tension. Geophysics 55:293–305

Vai GB (1979) Tracing the Hercynian structural zones across "Neo-Europa": an introduction. Mem Soc Geol It 20:39–45

Vannoli P, Basili R, Valensise G (2004) New geomorphic evidence for anticlinal growth driven by blind-thrust faulting along the northern Marche coastal belt (central Italy). J Seism 8:297–312

VIDEPI (2009) Visibilita dei dati afferenti all'attivita di esplorazione petrolifera in Italia. http://www.videpi.com

Wegmann KW, Pazzaglia FJ (2009) Late Quaternary fluvial terraces of the Romagna and Marche Apennines, Italy: climatic, lithologic, and tectonic controls on terrace genesis in an active orogen. Quat Sci Rev 28(2009):137–165

Wessel P, Smith WHF (1995) New version of Generic Mapping Tools (GMT) version 3.0 released. Eos Trans AGU 76:329

Williams SDP (2003) The effect of coloured noise on the uncertainties of rates estimated from geodetic time series. J Geod 76:483–494

Wilson LF, Pazzaglia FJ, Anastasio DJ (2009) A fluvial record of active fault-propagation folding, Salsomaggiore anticline, northern Apennines, Italy. J Geophys Res 114:B08403. doi:10.1029/2008JB005984

Winterer L, Bosellini A (1981) Subsidence and sedimentation on Jurassic passive continental margin, southern Alps Italy. AAPG Bull 65:394–421